Journal of Photochemistry and Photobiology A: Chemistry 201 (2009) 175–182

Contents lists available at ScienceDirect

Journal of Photochemistry and Photobiology A: Chemistry

journal homepage: www.elsevier.com/locate/jphotochem

Photoinduced electron transfer reactions of pyrylium derivatives with organic sulfides in acetonitrile

I. Sadhiya Banu, P. Ramamurthy*

National Centre for Ultrafast Processes, University of Madras, Taramani Campus, Chennai 600 113, India

ARTICLE INFO

Article history:
Received 6 June 2008
Received in revised form 28 October 2008
Accepted 29 October 2008
Available online 11 November 2008

Keywords:
Sensitiser
Fluorescence quenching
Electron transfer
Pyranyl radical

ABSTRACT

The photochemistry and photophysics of pyrylium derivatives with organic sulfides in acetonitrile medium are investigated. A steady decrease in the fluorescence intensity and fluorescence lifetime of the dyes was observed with increase in the quencher concentration. Bimolecular quenching constants were evaluated and correlated with the free energy of electron transfer. Laser flash photolysis investigations on the dyes in presence of quenchers were done. Observation of pyranyl radical and sulfide cation radicals as intermediates clearly illustrates the electron transfer mechanistic pathway for this reaction. The radical pair energies were calculated and found to be lower than the triplet energy of the sensitisers and hence we do not see any triplet induction in the present system.

1. Introduction

The intriguing progress made in the field of photoinduced electron transfer for the past few decades explicitly explains its potent importance in various emerging fields and still continues to be in focus of numerous theoretical and experimental investigations [1,2]. Electron transfer (ET) reactions in solution have been one of the most thoroughly investigated subjects in chemical reaction dynamics and major progress has been made on the dependence of ET rates on the free energy of reaction, on donor–acceptor distances as well as on the static properties of the solvents [3]. Marcus made a spectacular prediction applied to the relation between the free energy of activation and free energy of an electron transfer reaction and postulated the existence of "Marcus inverted region" (MIR) [4]. Vast research is being carried out till date on electron transfer reactions and MIR in various systems [5,6].

Pyrylium salts are well known electron transfer sensitisers in their excited singlet and triplet states. Many reports are available on the electron transfer reactions of these salts, more recently being in zeolites and ionic liquids [7,8]. More recently, Bonesi et al. [9] have reported the generation of radical ion promoted reaction of sulfides using pyrylium ions as photosensitisers. We have reported the excited state electron transfer reactions of 2,4,6-triphenylpyrylium ion [10] with various substituted benzene derivative donors in acetonitrile wherein, Marcus inverted behaviour was observed for the charge shift radical pair along with triplet induction with heavy atom containing donors. Triphenylpyrylium ion (TPP^+) in its excited state shows strong oxidizing property in contrast to the ground state as evidenced by its reduction potential values [11]. Pyrylium salts are positively charged substrates, wherein the electron transfer process with neutral donors produces only a charge exchange, generating the radical cation of the donor and the corresponding pyranyl radical. In this context, it is known that the formation of free radical ions enhances due to lack of columbic attraction and deactivation through back electron transfer (BET) is reduced [12]. We have already rationalized triplet induction due to presence of internal heavy atom in the probe [13] by carrying out the excited state electron transfer reactions of triphenylthiopyrylium ion with various substituted arene donors in acetonitrile. Wherein, the role of sulfur atom in probe in the recombination and the intersystem crossing rate constant was established.

The major aim of the present work is to understand the role of sulfur, a heavy atom in donors, in the electron transfer reaction with pyrylium salts. It should be noted that diarylcation radical of sulfonium salt is a key factor in cation polymerization using triaryl sulfonium salts. Specific one-electron oxidants are known to bring about oxidation of dialkyl sulfides R_2S leading to formation of sulfur-centered radical cations $R_2S^{\bullet+}$ [14]. These radical cations and their dimers have attracted considerable interest as possible intermediates in various enzymatic oxidants of organic sulfides [15].

* Corresponding author. Tel.: +91 44 24540962; fax: +91 44 24540709.
E-mail address: prm60@hotmail.com (P. Ramamurthy).

1010-6030/$ – see front matter © 2008 Elsevier B.V. All rights reserved.
doi:10.1016/j.jphotochem.2008.10.019

Herein, we report the excited state electron transfer reactions of three pyrylium derivatives with organic sulfide donors by carrying out the steady state and time resolved fluorescence quenching measurements. Bimolecular quenching constants were evaluated using time resolved fluorescence lifetime measurements for singlet quenching. Theoretical quenching constants were evaluated and correlated with experimental quenching constants. Laser flash photolysis experiments were carried out to monitor the transients formed in the above quenching process to further evidence the operation of electron transfer mechanism. The present work is a comparative study of the excited state reactions of pyrylium derivatives by varying the substitution along the *x*-chromophoric axis of the molecule and the pyrylium derivatives investigated in the present paper are

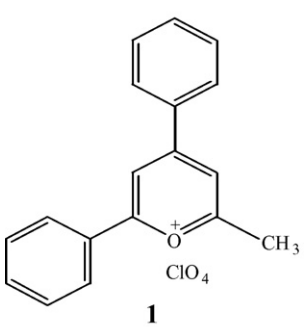

1

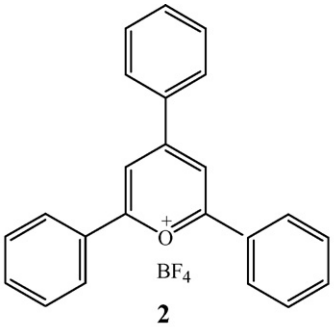

2

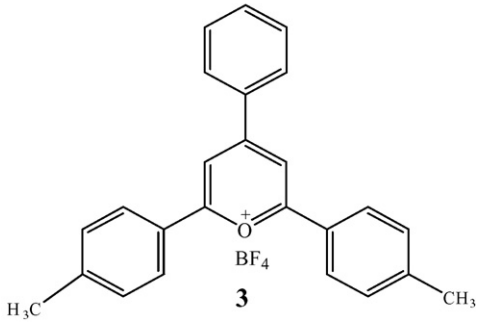

3

2. Experimental

2.1. Materials

2,4,6-Triphenylpyrylium tetrafluoroborate (**2**) was obtained from Aldrich and recrystallised before use. The synthesis and purification of 2-methyl-4,6-diphenylpyrylium perchlorate (**1**) and 2,6-di-*p*-tolyl-4-phenylpyrylium tetrafluoroborate (**3**) is given elsewhere [16]. All the quenchers were obtained from Lancaster India Pvt. Ltd., and used as such. Acetonitrile (spectroscopic grade) was obtained from Qualigens India Ltd., and used as received.

2.2. Instrumentation

Absorption spectra were recorded using Agilent 8543 diode-array spectrophotometer. Steady state fluorescence measurements of the dyes were carried out using the PerkinElmer MPF-44B fluorescence spectrophotometer interfaced with PC through RISHCOM-100 multimeter. The fluorescence decay measurements of the dye were carried out as reported elsewhere [17].

The reduction potentials and oxidation potentials of the dyes and sulfides and their respective diffusion coefficients were evaluated by electrochemical experiments. Cyclic voltammetric technique was adopted for the purpose. Cyclic voltammograms were recorded using a CHI-620B Electrochemical Analyzer, CH-Instruments Inc. About 10 ml of 1×10^{-3} M substrate in acetonitrile charged with tetrabutylammonium perchlorate was taken in an electrochemical cell and degassed by bubbling nitrogen for 15 min before the experiments.

A platinum disc working electrode, non-aqueous Ag/AgCl reference electrode and platinum wire counter electrode were employed for the CV experiments. Voltammograms were recorded at various scan rates from 10 to 1000 mV/s and employing the peak current values diffusion coefficients for the analytes were evaluated.

Laser flash photolysis experiments were carried out using the third harmonic (355 nm) output from Quanta Ray Lab-150 (Spectra Physics) Nd-YAG laser with a pulse width of 8 ns and energy around 150 mJ. The monitoring light source was a 150 W pulsed Xe lamp, focused on sample at 90° to incident laser beam. The source beam emerging through the sample was focused on to a Czerney–Turner monochromator using a pair of lenses. The detection was carried out using a Hamamatsu R-928 photomultiplier tube. The transient signals were captured with a Agilent infinium 54810A digital storage oscilloscope and transferred to a computer.

3. Results and discussion

3.1. Fluorescence quenching studies—steady state and time resolved

The absorption and emission spectra of the dyes were recorded in the presence and absence of quenchers and it is observed that the absorption spectral shape of the dyes remains the same in the absence and presence of quenchers. However, a steady decrease in the fluorescence intensity and fluorescence lifetime with increase in quencher concentration is observed (Fig. 1.) which is illustrative of an excited state reaction of the dyes with the donors. Bimolecular quenching constants were evaluated following a linear Stern–Volmer relationship [18], which is indicative of a dynamic quenching process in case of **2** and **3** (Fig. 2a).

$$\frac{I_0}{I} = 1 + K_{sv}[Q] \quad (1)$$

$$\frac{\tau_0}{\tau} = 1 + k_q \tau_0 [Q] \quad (2)$$

where I_0 and I are the fluorescence intensities of the dye in the absence and presence of donors and τ_0 and τ are the fluorescence lifetime of dyes in the absence and presence of donors and k_q is the quenching constant obtained. However the Stern–Volmer plot of **1** shows a linear increase only at low quencher concentrations and later shows a positive deviation at higher concentrations (Fig. 2a). An upward curvature in the SV plot is indicative of the simultaneous participation of static and dynamic quenching process in present system.

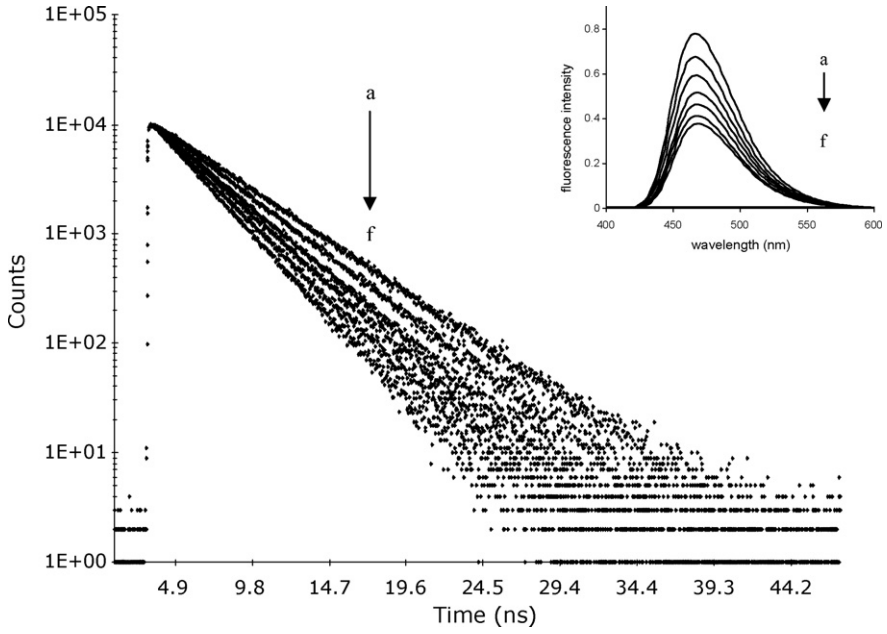

Fig. 1. Fluorescence lifetime quenching of **2** (1×10^{-5} M) in presence of DPS: (a) 0 M; (b) 1.68×10^{-3} M; (c) 3.36×10^{-3} M; (d) 5.02×10^{-3} M; (e) 6.68×10^{-3} M; (f) 8.33×10^{-3} M [inset: steady state fluorescence quenching].

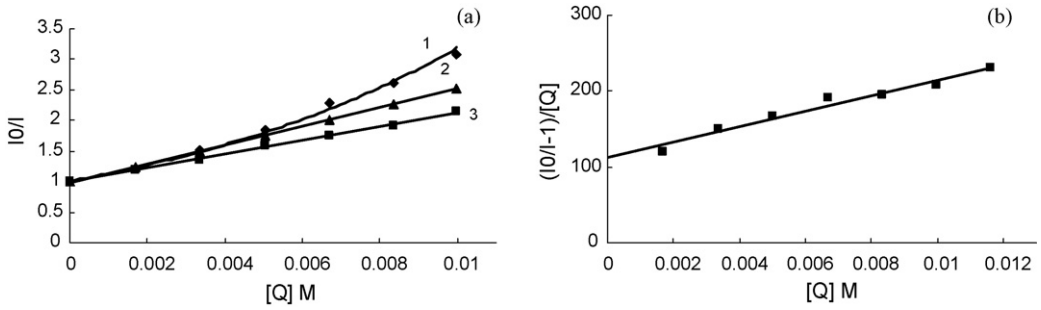

Fig. 2. (a) Stern–Volmer plots for steady-state fluorescence quenching of **1**, **2** and **3** in presence of methyl-*p*-tolyl sulfide. (b) Modified Stern–Volmer plot for **1** in presence of methyl-*p*-tolyl sulfide.

3.2. Free energy correlation

The free energy change associated with the electron transfer was calculated using the Rehm–Weller expression (Eq. (3)).

$$\Delta G_{et} = E_{1/2\,oxd.} + E_{1/2\,red.} - E_{(0,0)} + C \quad (3)$$

where $E_{1/2\,oxd.}$ is the oxidation potential of the donors, $E_{1/2\,red.}$ the reduction potential of dye, $E_{(0,0)}$ the singlet state energy of the sensitiser and C is the columbic energy term. Since one of the reactant used is neutral, pyrylium salts are charged and the solvent used is polar, there will be no net change of charge upon electron transfer and the contribution of this term is ignored here [19]. The bimolecular quenching constants for all the dyes were evaluated and correlated with the free energy change associated with the electron transfer reactions and presented in Tables 1–3.

Table 1
Experimental and theoretical quenching constants of **1**.

Quencher	ΔG_{et}[a] (eV)	$E_{1/2\,oxd.}$[a] (V)	K_a[a] (M^{-1})	$k_q \times 10^{-10}$ M^{-1} s^{-1} lifetime derived[a]	ΔG (kcal M^{-1})	Debye[b] $k_q \times 10^{-10}$ M^{-1} s^{-1}	Smoluchowskii[c] $k_q \times 10^{-10}$ M^{-1} s^{-1}
Methyl-*p*-tolyl sulfide	−1.10	1.57	25.6	2.47	0.2251	1.49	2.67
Methylphenyl sulfide	−1.04	1.63	26.5	2.46	0.2378	1.49	2.65
Diphenyl sulfide	−0.98	1.69	27.6	2.30	0.2447	1.48	2.51
Ethylphenyl sulfide	−0.95	1.72	33.6	2.23	0.2521	1.48	2.48
Phenyl-*n*-propyl sulfide	−0.93	1.74	37.9	2.17	0.2598	1.47	2.28
Diethyl sulfide	−0.71	1.96	39.3	2.04	0.3445	1.41	1.70
Di-*n*-propyl sulfide	−0.70	1.97	48.8	1.90	0.3493	1.41	1.72
Di-*n*-butyl sulfide	−0.69	1.98	53.9	1.75	0.3541	1.41	1.55
Di-*t*-butyl sulfide	−0.69	1.99	53.7	1.76	0.3584	1.41	1.56

[a] Experimental k_q values calculated using $E_{1/2\,red} = -0.41$ eV, $E_{(0,0)} = 3.08$ eV and $D_f = 3.21 \pm 0.3 \times 10^{-5}$ cm^2 s^{-1}.
[b] Theoretical k_q calculated using $k_d = 2 \times 10^{10}$ M^{-1} s^{-1} (Debye equation).
[c] Theoretical k_q calculated using $k_d = 4.35 \times 10^{10}$ M^{-1} s^{-1} (Smoluchowskii equation).

Table 2
Experimental and theoretical quenching constants of **2**.

Quencher	ΔG_{et}[a] (eV)	$E_{1/2\,oxd.}$[a] (V)	$k_q \times 10^{-10}$ M^{-1} s^{-1} steady state derived[a]	$k_q \times 10^{-10}$ M^{-1} s^{-1} lifetime derived[a]	ΔG (kcal M^{-1})	Debye[b] $k_q \times 10^{-10}$ M^{-1} s^{-1}	Smoluchowskii[c] $k_q \times 10^{-10}$ M^{-1} s^{-1}
Methyl-*p*-tolyl sulfide	−1.02	1.57	3.6	2.50	0.2424	1.48	2.53
Methylphenyl sulfide	−0.96	1.63	3.31	2.34	0.2572	1.47	2.51
Diphenyl sulfide	−0.90	1.69	3.13	2.04	0.2625	1.46	2.36
Ethylphenyl sulfide	−0.87	1.72	3.00	2.08	0.2739	1.46	2.34
Phenyl-*n*-propyl sulfide	−0.84	1.74	2.96	2.08	0.2831	1.47	2.13
Diethyl sulfide	−0.63	1.96	2.64	1.88	0.3862	1.38	1.70
Di-*n*-propyl sulfide	−0.62	1.97	2.60	1.73	0.3921	1.38	1.72
Di-*n*-butyl sulfide	−0.61	1.98	2.54	1.71	0.3982	1.38	1.55
Di-*t*-butyl sulfide	−0.69	1.99	53.7	1.76	0.4045	1.37	1.56

[a] Experimental k_q values calculated using $E_{1/2\,red} = -0.21$ eV, $E_{(0,0)} = 2.80$ eV and $D_f = 2.58 \pm 0.3 \times 10^{-5}$ cm^2 s^{-1}.
[b] Theoretical k_q calculated using $k_d = 2 \times 10^{10}$ M^{-1} s^{-1} (Debye equation).
[c] Theoretical k_q calculated using $k_d = 4.01 \times 10^{10}$ M^{-1} s^{-1} (Smoluchowskii equation).

Table 3
Experimental and theoretical quenching constants of **3**.

Quencher	ΔG_{et}[a] (eV)	$E_{1/2\,oxd.}$ (V)[a]	$k_q \times 10^{-10}$ M^{-1} s^{-1} steady state derived[a]	$k_q \times 10^{-10}$ M^{-1} s^{-1} lifetime derived[a]	ΔG (kcal M^{-1})	Debye[b] $k_q \times 10^{-10}$ M^{-1} s^{-1}	Smoluchowskii[c] $k_q \times 10^{-10}$ M^{-1} s^{-1}
Methyl-*p*-tolyl sulfide	−0.87	1.57	4.03	2.25	0.2831	1.46	2.24
Methylphenyl sulfide	−0.81	1.63	3.43	2.17	0.3034	1.44	2.21
Diphenyl sulfide	−0.75	1.69	3.13	1.96	0.3269	1.43	2.17
Ethylphenyl sulfide	−0.72	1.72	3.17	1.85	0.3399	1.42	2.15
Phenyl-*n*-propyl sulfide	−0.70	1.74	3.47	1.86	0.3492	1.41	2.14
Diethyl sulfide	−0.48	1.96	3.22	1.57	0.4979	1.30	1.89
Di-*n*-propyl sulfide	−0.47	1.97	2.97	1.41	0.5077	1.29	1.88
Di-*n*-butyl sulfide	−0.46	1.98	2.61	1.47	0.5177	1.29	1.86
Di-*t*-butyl sulfide	−0.45	1.99	2.97	1.35	0.5281	1.28	1.85

[a] Experimental k_q values calculated using $E_{1/2\,red} = -0.27$ eV, $E_{(0,0)} = 2.71$ eV and $D_f = 2.27 \pm 0.05 \times 10^{-5}$ cm^2 s^{-1}.
[b] Theoretical k_q calculated using $k_d = 2 \times 10^{10}$ M^{-1} s^{-1} (Debye equation).
[c] Theoretical k_q calculated using $k_d = 3.85 \times 10^{10}$ M^{-1} s^{-1} (Smoluchowskii equation).

From the data obtained it could be seen that the steady state quenching constants are higher than the lifetime quenching constants for **2** and **3**. The deviation could be well explained in terms of combined static and dynamic quenching effect [20,21]. The observation of an upward curvature in the Stern–Volmer plot of **1** also evidences the presence of such a combined static and dynamic quenching process taking place in the present study. The linearity in the Stern–Volmer plots for systems **2** and **3** suggests that the fluorophore and quencher are only weakly associated in these systems in the observed concentration range. On the other hand, for **1** the deviation is observed only at higher quencher concentrations suggesting that the fluorescer and quencher do not actually form ground state complex. Rather, the static quenching here presumes that the dye and the quencher exist as closed contact pair in solution without any complex formation and quenching of the fluorescence of dye in such a case takes place instantaneously upon excitation of the sample. Reports are available on systems exhibiting both types of quenching [22] and are found to obey the modified Stern–Volmer equation (Eq. (4)).

$$\frac{I_0}{I} = 1 + (K_a K_{sv})[Q] + K_a K_{sv}[Q]^2 \quad (4)$$

where K_a is the association constant and K_{sv} the Stern–Volmer constant ($K_{sv} = k_q \tau_0$). Since no new peak appeared in the absorption or fluorescence spectrum of **1** upon addition of donor, the experimental data was fitted into modified SV plot (Fig. 2b). The association constants were obtained by combining the time resolved and steady state intensity measurements.

A plot of $(I_0/I - 1)/[Q]$ vs. $[Q]$ gives $(K_a + K_{sv})$ as intercept and $K_{sv}K_a$ as the slope. Taking the K_{sv} values from the time resolved Stern–Volmer plot (Eq. (2)) K_a values were evaluated and are tabulated in Table 1.

3.3. Theoretical quenching constants evaluation—deviations with experimental values

The overall theoretical quenching constants were evaluated following the given expression (Eq. (5)).

$$k_q = \frac{k_d}{(1 + (k_d/K_D A)\,[\exp(\Delta G_{et}/RT) + \exp(\Delta G^{\#}/RT)])} \quad (5)$$

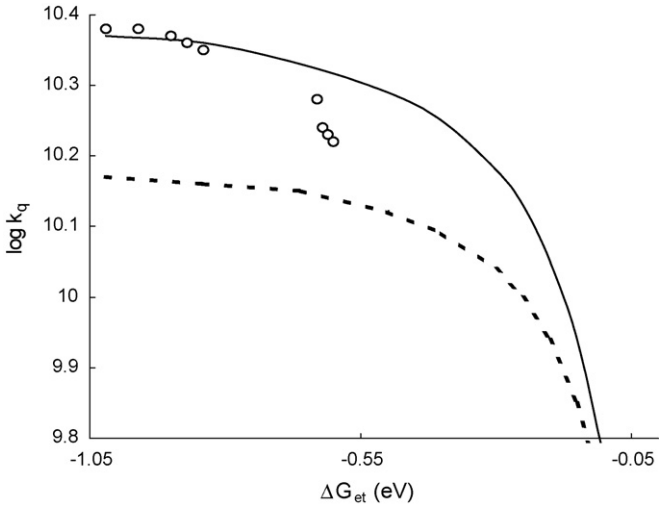

Fig. 3. Plot of $\log k_q$ vs. ΔG_{et} for **2**: (○) lifetime derived experimental $\log k_q$ values; (–) theoretical $\log k_q$ values calculated using $k_d = 2 \times 10^{10}$ M^{-1} s^{-1} as obtained from Debye equation; (—) using $k_d = 4.01 \times 10^{10}$ M^{-1} s^{-1} as obtained from Smoluchowskii equation.

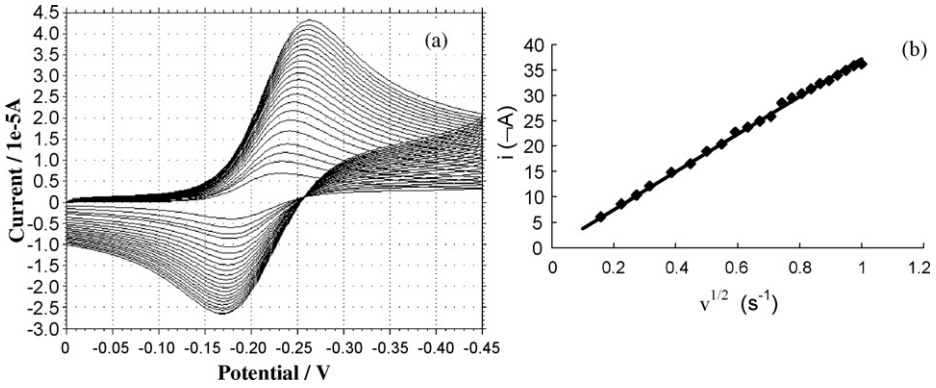

Fig. 4. (a) Cyclic voltammogram of **2** (1.01×10^{-3} M) in presence of supporting electrolyte tetrabutylammonium perchlorate (0.1 M) using platinum working electrode, non-aqueous Ag/AgCl reference electrode and platinum counter electrode at various scan rates from 10 to 1000 mV/s (b) plot of i (μA) vs. $v^{1/2}$ (s^{-1}).

where K_D is the equilibrium diffusion constant ($K_D = k_d/k_{-d}$) and value of 0.865 is estimated when the distance of two molecules is 7 Å [23]. k_d and k_{-d} are the diffusion and dissociation rate constants. A is the effective collision frequency and a value of 1×10^{11} s^{-1} was employed [24] in the calculation of k_q. $\Delta G^{\#}$ is the free energy of activation for electron transfer. ΔG_{et} is the free energy of electron transfer. The free energy of activation was calculated using Rehm–Weller [25] treatment (Eq. (6)).

$$\Delta G^{\#} = \frac{\Delta G_{et}}{2} + \left[\left(\frac{(\Delta G_{et})}{2}\right)^2 + (\Delta G_0^{\#})^2\right]^{1/2} \quad (6)$$

where $\Delta G_0^{\#}$ is the free energy of activation in the absence of driving force and a value of 2.4 kcal M^{-1} is employed as according to Rehm–Weller [25]. The overall quenching constant values were calculated by using the k_d value of 2×10^{10} M^{-1} s^{-1} as obtained by the Debye expression [26] (Eq. (7)).

$$k_d = \frac{8000RT}{3\eta} \quad (7)$$

where η is the solvent viscosity (in units of Pascal second and a value of 0.325 was used [27]), R and T have their usual meanings. k_{-d} is rate of dissociation of the precursor complex and was estimated from Eigen equation [28] for reactants with no Columbic interaction. Theoretical quenching constants were calculated for all three dyes. The theoretical quenching constants (k_q) obtained using Rehm–Weller [25] treatment is plotted ($\log k_q$) against ΔG_{et} (Fig. 3.) for **2**. The figure shows poor correlation with the lifetime derived experimental values and the calculated k_q values are given in the tables.

The calculated quenching constants are found to be lower than the experimental ones. The cause of such deviation of k_q values is in the approximation of k_d values. The Debye expression used in the calculation of k_d includes temperature and viscosity parameters and is applicable only to molecules of comparable size with the solvent molecules. It is known that diffusion can limit the rate of electron transfer. Since pyrylium moiety is charged and larger in size, k_d value has to be found from the diffusion measurements which would account for the radius of the molecules. The k_d values were then calculated using Smoluchowskii equation [29] (Eq. (8)).

$$k_d = 4\pi N(D_f + D_q)a \quad (8)$$

where D_f and D_q are the diffusion coefficients of the fluorescer and quencher, respectively.

3.4. Electrochemical measurements

The diffusion coefficients of both fluorescer and quencher were determined experimentally using cyclic voltammetric technique by making use of Randels–Sevcik equation (Eq. (9)).

$$i = (2.687 \times 10^5)n^{3/2}v^{1/2}D^{1/2}AC \quad (9)$$

where n is the number of electrons involved in the electrochemical reaction (=1), D the diffusion coefficient (in units of cm^2 s^{-1}), ν the

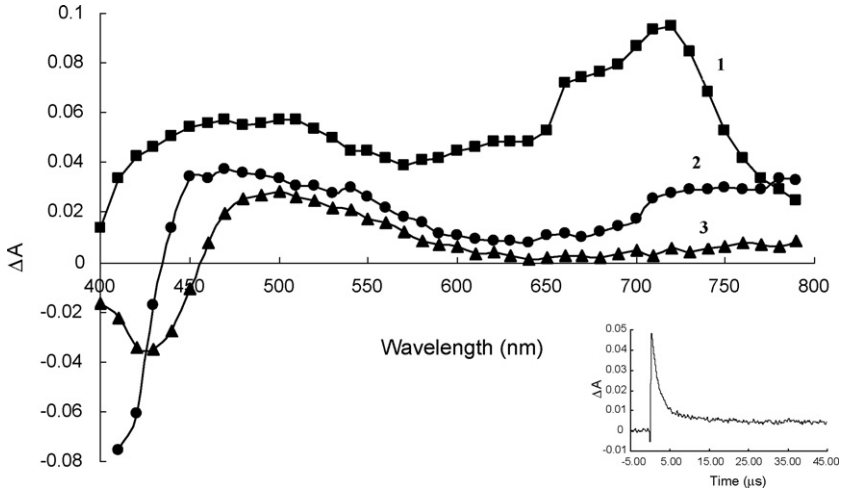

Fig. 5. Transient absorption spectrum of **1**, **2** and **3** (4.8×10^{-5} M) after 1 μs of laser pulse at 355 nm in acetonitrile [inset: transient decay monitored at 470 nm for **2**].

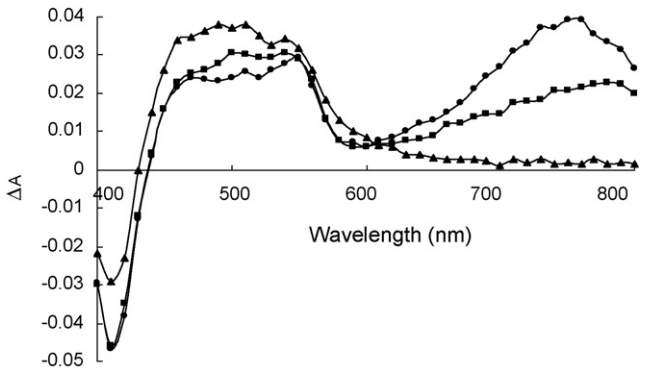

Fig. 6. Transient absorption spectrum of **2** in presence of (●) DPS, (■) MPS and (▲) DES after 2 μs of laser pulse at 355 nm (**2** = 4.8×10^{-5} M, DPS = 36 mM, MPS = 34 mM and DES = 37 mM) in acetonitrile.

scan rate (in units of s^{-1}), A the area of the electrode (in units of cm) and C is the concentration of the analyte. The voltammograms were recorded at various scan rates initiating from 10 to 1000 mV/s. The corresponding voltammograms recorded for **2** are outlined in Fig. 4a. Both the oxidation and reduction peak current increases with the increase in scan rates. Plot of reduction peak current against square root of scan rate (Fig. 4b) illustrates a linearity in the scan range examined which is indicative of the diffusion controlled process of electron transfer at the electrode surface. From the slope of the curve, the diffusion coefficients of the analyte were determined. For **2** and **3**, the curves were reversible whereas for **1** and for the quenchers the voltammograms were irreversible. The reason for the irreversible nature for **1** is due to the rapid irreversible dimerisation of the radical formed. Hence, the peak potentials were used as $E_{1/2\,red.}$ for **1** and $E_{1/2\,oxd.}$ for the sulfides in the calculation of ΔG_{et} and diffusion coefficients.

The diffusion coefficients evaluated by above technique are given in Tables 1–3. The diffusion coefficient for the series of sulfides was calculated to be $5 \pm 0.5 \times 10^{-5}$ cm^2 s^{-1}. The k_d value thus obtained by substituting these diffusion coefficients in Smoluchowskii equation are also tabulated. The k_q values calculated using obtained k_d value shows fairly good agreement with the lifetime derived experimental k_q values for the Rehm–Weller treatment in all the three cases as seen from Tables 1–3. A plot of $\log k_q$ vs. ΔG_{et} (Fig. 3) for **2** also shows a good correlation. This explains the diffusion-controlled nature of the electron transfer and marks a proof for the excited state electron transfer reaction in these systems.

It can be seen that the experimental k_q values for the alkyl sulfides are lower when compared to the aromatic sulfides. This is due to the fact that, the electron transfer rates are directly related to the shapes of the highest occupied molecular orbitals (HOMO) of the donors. Aromatic sulfides are π-type donors and aliphatic sulfides are of n-type. For aromatic sulfides, the lone pair of electrons on the sulfur atom is fairly delocalised over the entire molecule and the HOMO for these molecules has a π-type character. Whereas, for aliphatic sulfides no such aromatic π cloud in resonance with the lone pair is present and hence the HOMO of these molecules are more of n-type and hence show lower quenching constant values [30].

3.5. Laser flash photolysis studies

Laser flash photolysis (λ_{exc} = 355 nm) studies of Argon purged samples of all the dyes in acetonitrile was carried out. The transient absorption spectrum of all the three dyes in the absence of sulfides after 1 μs of laser pulse is shown in Fig. 5. The absorption spectrum is characterised by a maximum at 470 nm for **2** and **3**, which is assigned to the triplet state in accordance with the earlier observations [10]. On the other hand, fluorophore **1** shows a broad transient in the region 450–550 nm and another at 720 nm where both can be assigned as triplet absorption.

3.5.1. Radical cations of sulfides

Fig. 6 shows the transient absorption of **2** in presence of diphenyl sulfide (DPS), methylphenyl sulfide (MPS) and diethyl sulfide (DES) after 2 μs of laser pulse. In the absence of DPS, the triplet at 470 nm obeys first order kinetics and has a lifetime of about 2.8 μs. In presence of DPS, the transient spectrum exhibits a broad maximum in the region 470–550 nm assigned to the triplet and pyranyl radical of **2**, a broad transient in the wavelength region 700–800 nm with a maximum around 740 nm which is characteristic of $DPS^{\bullet+}$ and a strong bleaching below 450 nm. This is in agreement with the reports mentioned elsewhere [10,31,32]. Sawaki et al. [31] have demonstrated in their earlier experiments that the radical cations of aromatic sulfides (DPS) do not form any dimer as expected for other aliphatic sulfides (which are stabilised by forming dimers) because of the delocalisation of positive charge/spin density over the aromatic rings. Early literature reports on DPS [33,34] also suggest that $DPS^{\bullet+}$ does not form dimer and the monomer radical cation absorbs around 740 nm.

Fig. 7 shows the transient decays monitored at 470 and 740 nm for **2** in the absence and presence of DPS. Wherein, a decrease in triplet absorption at 470 nm of **2** in presence of DPS with no appreciable change in lifetime (2.6 μs) and observation of $DPS^{\bullet+}$ transient at 740 nm is seen. At 740 nm in presence of DPS, the transient obeys first order kinetics and has a lifetime of about 15 μs. The transients observed at 740 nm in the absence and presence of DPS have different rate constants (2.2×10^4 s^{-1} and 6.3×10^4 s^{-1}) and hence are two different species observed. Sawaki and coworkers have already rationalized the observation of $DPS^{\bullet+}$ at 740 nm in their earlier experiments [31]. The transient observed at 740 nm in the presence of DPS in our experiments clearly supports this observation and hence could be safely assigned as the $DPS^{\bullet+}$.

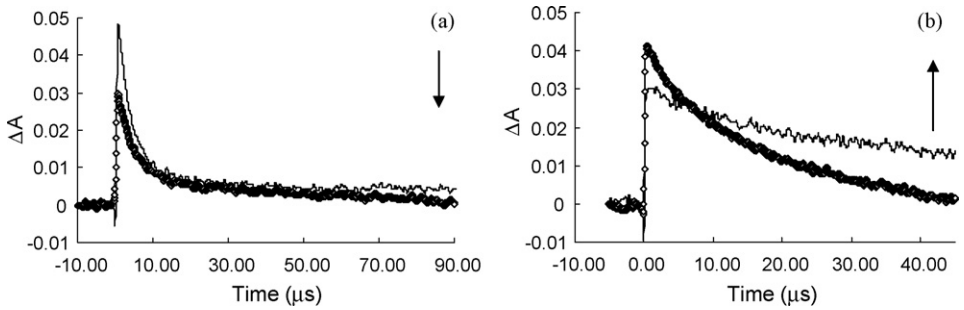

Fig. 7. Transient decays of **2** in (—) absence and (◊) presence of DPS monitored at (a) 470 nm and (b) 740 nm (**2** = 4.8×10^{-5} M and DPS = 36 mM) in acetonitrile.

It is also mentioned in the literature [31] that MPS can form both monomer as well as dimer radical cations depending upon its concentration. The MPS monomer radical cation absorbs only at 520 nm and the dimer radical cation absorbs around 520 nm as well as around 800 nm. Fig. 6 shows a broad transient absorption in the region 650–800 nm with a maximum around 780 nm in presence of MPS. The transient at 780 nm in presence of MPS obeys first order kinetics and has a lifetime about 25 μs. In addition, rate constants of the decays at 780 nm in the absence and presence of MPS are $1.5 \times 10^5\ s^{-1}$ and $4.04 \times 10^4\ s^{-1}$, respectively. This clearly explains the fact that both are two different transients observed. Hence, it could be suggested that the transient observed around 780 nm in presence of MPS is due to the occurrence of stable dimer radical cations of methylphenyl sulfide upon electron transfer in the observed concentration range of MPS.

In Fig. 6, the 740 nm peak is not seen in presence of the aliphatic sulfides like diethyl sulfide (DES). Rather, the transient absorption spectrum shows a broad absorption band in the region 450–560 nm with a maximum around 490 nm. This is also in agreement with the literature report by Sawaki et al. [31], which states that, the radical cations of aliphatic organic sulfides form σ- and π-type dimers depending on their substitution and exhibits a transient maximum around 490 nm. The rate constant of the transient monitored at 490 nm in the absence of DES is $3.0 \times 10^5\ s^{-1}$ with lifetime of about 3.2 μs. In presence of DES is the transient decay undergoes biexponential fit with lifetimes of about 2.48 and 30 μs (the relative amplitudes are 13 and 87%). The biexponential behaviour of the transient suggests the presence of both triplet of **2** and the dimer radical cation of DES. The observation of a broad transient absorption band around 450–560 nm with a maximum around 490 nm indicates the formation of dimer radical cation of DES as $(DES)_2^{\bullet+}$ which is found to occur along with the triplet in this wavelength region as seen in Fig. 6.

Our earlier experiments with pyrylium ion using benzene derivatives as quenchers [10] triplet induction was observed in presence of heavy atom containing donors like iodobenzene, bromobenzene, bromotoluene, etc. due to the spin orbit coupling of the heavy atom present in the donors. No triplet induction was observed for quenchers without heavy atom despite their radical pair energies being higher than triplet energy of sensitiser. On the other hand, experiments with thiopyrylium analogue [13] having an internal heavy atom sulfur in the ring showed triplet induction for all the arene quenchers with radical pair energy higher than the triplet energy of sensitiser due to enhancement in the intersystem crossing rate constant as a result of homocyclic heavy atom spin-orbit coupling. In the present system, the radical pair energies were calculated and found to be lower than the triplet energy of the sensitiser. Since the radical pair energies are lower than the triplet energy of the sensitisers, singlet to triplet geminate radical pair formation and hence charge recombination leading to triplet state formation becomes impossible based on energetics grounds. Hence, we do not see any triplet induction in all the three dyes. The calculated radical pair energies for **2** are tabulated in Table 4. Similar results were also obtained for compounds **1** and **3**.

3.5.2. *Pyranyl radical (TPP•)*

We observed the formation of pyranyl radical of the sensitisers in presence of all the sulfides. Fig. 8 shows the transient absorption spectrum of **2** in presence of DPS after 35 μs of laser pulse characterised by a maximum at 550 nm. Following the literature reports [10] the 550 nm absorption is assigned to the pyranyl radical (**2•**) generated due to electron transfer from quencher (DPS). Formation of pyranyl radical (**2•**) was further evidenced by a similar absorption spectrum obtained by the chemical reduction of **2** using Zn dust [35] (inset in Fig. 8). Similar results were obtained for compounds **1** and **3** also. Where the radical of **1** shows a transient absorption at 500 nm and the radical of **3** show a transient absorption at 550 nm similar to **2•**. Fig. 9 shows the transient decay of **2** monitored at 550 nm in the absence of DPS and the pyranyl radical observed in presence of DPS after 30 μs of laser pulse. The pyranyl radical observed at 550 nm obeys first order kinetics and has a lifetime of 35 μs. As evidenced from Fig. 9, it could be suggested that the pyrany radical yield is very low in the present system of electron transfer.

Table 4
The radical pair energies of **2**[a].

Quencher	$E_{1/2\,oxd.}$ (V)[a]	$\Delta G_{(rp)}$[b]
Methyl-*p*-tolyl sulfide	1.57	1.78
Methylphenyl sulfide	1.63	1.84
Diphenyl sulfide	1.69	1.90
Ethylphenyl sulfide	1.72	1.93
Phenyl-*n*-propyl sulfide	1.74	1.95
Diethyl sulfide	1.96	2.17
Di-*n*-propyl sulfide	1.97	2.18
Di-*n*-butyl sulfide	1.98	2.19
Di-*t*-butyl sulfide	1.99	2.20

[a] Triplet energy of the sensitiser = 2.30 eV.
[b] $\Delta G_{(rp)} = E_{1/2\,oxd.} - E_{1/2\,red}$.

In order to investigate the presence of Marcus inverted region in back electron transfer reactions the pyranyl radical yield were calculated [36] and found to be very low as compared to our earlier experiments with arene derivatives [10]. Further, the experimental back electron transfer rate constants (k_b) were also evaluated using

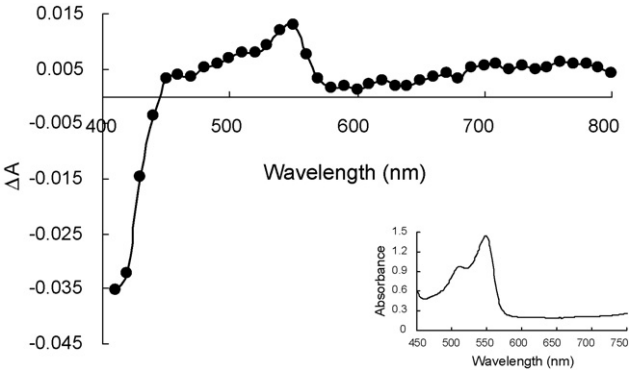

Fig. 8. Transient absorption spectrum of **2** in presence of DPS after 35 μs of laser pulse at 355 nm (**2** = 4.8×10^{-5} M and DPS = 36 mM) in acetonitrile [inset: absorption spectrum of **2•** obtained by chemical reduction of **2**].

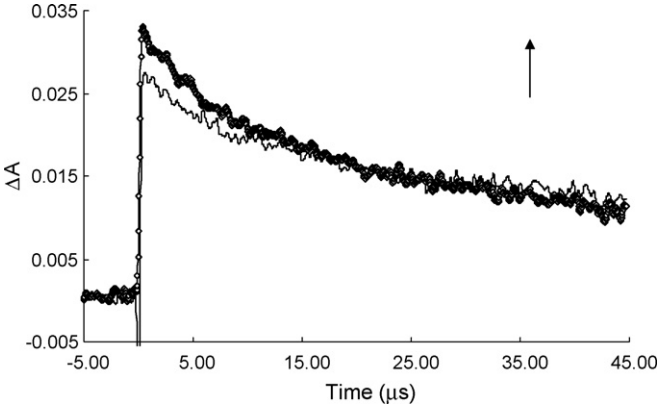

Fig. 9. Transient decays of **2** in (—) absence and (◊) presence of DPS monitored at 550 nm (**2** = 4.8×10^{-5} M, DPS = 36 mM) in acetonitrile.

the following expression (Eq. (10)).

$$\phi_r = \frac{k_{esc}}{k_{esc} + k_b} \quad (10)$$

The well-known semi classical expression [37] was used for the calculation of theoretical back electron transfer rate constants (k_b). Only few data points could be evaluated for experimental k_b values due to poor radical yield and the experimental k_b values lie in the inverted region in the plot of $\log k_b$ vs. ΔG_b.

4. Conclusion

Fluorescence quenching of pyrylium derivatives was carried out using organic sulfide quenchers in acetonitrile medium. Observation of no characteristic change in absorption spectral shapes and a steady decrease in the fluorescence intensity and fluorescence lifetimes of the fluorophores suggests an excited state reaction between the dyes and quenchers. Correlation of free energy of electron transfer to the bimolecular quenching constants proves the excited state reaction to be photoinduced electron transfer reaction. Poor correlation of the theoretical quenching constants with the experimental ones using diffusion constant obtained from Debye equation was observed. Good correlation upon using diffusion constant obtained from Smoluchowskii equation evidences the presence of diffusion controlled excited state electron transfer reaction of the dyes with the sulfides. The observation of triplet state, pyranyl radical and sulfide cation radicals as transients in laser flash photolysis experiments also clearly supports this illustration. The radical pair energies were calculated and found to be lower than the triplet energy of the sensitiser. Hence, we do not see triplet induction in all the three dyes.

Acknowledgement

The authors sincerely acknowledge the financial support rendered by the Council of Scientific and Industrial Research (CSIR), Government of India.

Appendix A. Supplementary data

Supplementary data associated with this article can be found, in the online version, at doi:10.1016/j.jphotochem.2008.10.019.

References

[1] L. Eberson, Adv. Phys. Org. Chem. 18 (1982) 79–185.
[2] G.J. Kavarnos, N.J. Turro, Chem. Rev. 86 (1986) 401–449.
[3] H. Heitele, Angew. Chem. Int. Ed. Engl. 32 (1993) 359–377.
[4] R.A. Marcus, J. Chem. Phys. 24 (1956) 966–979.
[5] P. Sun, F. Li, Y. Chen, M. Zhang, Z. Zhang, Z. Gao, Y. Shao, J. Am. Chem. Soc. 125 (2003) 9600–9601.
[6] A.G. Griesbeck, N. Hoffmann, K.D. Warzecha, Acc. Chem. Res. 40 (2007) 128–140.
[7] M. Alvaro, E. Carbonell, H. Garcia, C. Lamaza, M.N. Pillai, Photochem. Photobiol. Sci. 3 (2004) 189–193.
[8] S. Marquis, B. Ferrer, M. Alvaro, H. Garcia, H.D. Roth, J. Phys. Chem. B 110 (2006) 14956–14960.
[9] S.M. Bonesi, E. Carbonell, H. Garcia, M. Fagnoni, A. Albini, Appl. Catal. B. Environ. 79 (2008) 368.
[10] S.S. Jayanthi, P. Ramamurthy, J. Phys. Chem. A 101 (1997) 2016–2022.
[11] V. Wintgens, J. Pouliquen, J. Kossanyi, Nouv. J. Chim. 9 (1985) 229–234.
[12] M.A. Miranda, H. Garcia, Chem. Rev. 94 (1994) 1063–1089.
[13] S.S. Jayanthi, P. Ramamurthy, J. Phys. Chem. A 102 (1998) 511–518.
[14] J. Monig, R. Goslich, K.-D. Asmus, J. Phys. Chem. 90 (1986) 115–121.
[15] C. Schoneich, K.-D. Asmus, M. Bonifacic, J. Chem. Soc., Faraday Trans. 91 (1995) 1923–1930.
[16] J.A. Van Allan, P.G.A. Reynolds, J. Org. Chem. 33 (1968) 1102–1105.
[17] R. Kumaran, P. Ramamurthy, J. Phys. Chem. B 110 (2006) 23783–23789.
[18] N.J. Turro, Modern Molecular Photochemistry, Benjamin Cumings, Menlopark, CA, 1978.
[19] P. Ramamurthy, S. Parret, F.M. Savary, J.P. Fouassier, J. Photchem. Photobiol. A 83 (1994) 205–209.
[20] P. Drossler, W. Holzer, A. Penzkofer, Hegemann, Chem. Phys. 286 (2003) 409–420.
[21] M.R. Eftink, C.A. Ghiron, J. Phys. Chem. 80 (1976) 486–493.
[22] E.Y. Komarova, K. Ren, D.C. Neckers, J. Phys. Chem. 107 (2003) 5675–5679.
[23] L. Eberson, in: V. Gold, D. Bhell (Eds.), Advances in Physical Organic Chemistry, Academic Press, New York, 1982.
[24] G.L. Hug, B. Marciniak, J. Phys. Chem. 99 (1995) 1478–1483.
[25] D. Rehm, A. Weller, Isr. J. Chem. 8 (1970) 259–271.
[26] J. Sattiel, B.W. Atwater, in: D.H. Volmas, G.S. Hammond, K. Gollaick (Eds.), Advances in Photochemistry, Wiley, New York, 1988.
[27] T. Niwa, K. Kikuchi, N. Matsusita, M. Hayashi, T. Katagiri, Y. Takahashi, T. Miyashi, J. Phys. Chem. 97 (1993) 11960–11964.
[28] M. Eigen, Z. Phys. Chem. 203 (1954) 176–200.
[29] M. Smoluchowskii, J. Phys. Chem. 92 (1917) 129–168.
[30] P. Jacques, X. Allonas, Chem. Phys. Lett. 233 (1995) 533–537.
[31] H. Yokoi, A. Hatta, K. Ishiguro, Y. Sawaki, J. Am. Chem. Soc. 120 (1998) 12728–12733.
[32] C. Selvaraju, A. Sivakumar, P. Ramamurthy, J. Photochem. Photobiol. A: Chem. 138 (2001) 213–226.
[33] S.A. Chaudhri, H. Mohan, E. Anklam, K.-D. Asmus, J. Chem. Soc. Perkin. Trans. 2 (1996) 383–390.
[34] M.A. James, M.L. McKee, A.J. Illies, J. Am. Chem. Soc. 118 (1996) 7836–7842.
[35] V. Wintgens, J. Pouliquen, J. Kossanyi, Nouv. J. Chim. 10 (1986) 345–350.
[36] P. Iwa, V. Steiner, E. Vogelmann, H.E.A. Kramer, J. Phys. Chem. 86 (1982) 1277–1285.
[37] D. Burget, P. Jaques, E. Vauthey, P. Suppan, E. Haselbach, J. Chem. Soc., Faraday Trans. 90 (1994) 2481–2487.